

An efficient post-processing technique for fabricating SNAP microresonators with sub-angstrom precision by femtosecond laser

QI YU,¹ YUEQING DU,¹ ZUOWEI XU,¹ PENG WANG,¹ ZHEN ZHANG,¹ ZECE ZHU,¹ HAORAN CAO,¹ MICHAEL SUMETSKY,² AND XUEWEN SHU^{1,*}

¹Wuhan National Laboratory for Optoelectronics & School of Optical and Electronic Information, Huazhong University of Science and Technology, Wuhan 430074, China

²Aston Institute of Photonic Technologies, Aston University, Birmingham B4 7ET, UK

*Corresponding author: xshu@hust.edu.cn

Received XX Month XXXX; revised XX Month, XXXX; accepted XX Month XXXX; posted XX Month XXXX (Doc. ID XXXXX); published XX Month XXXX

We demonstrated the sub-angstrom precise correction of surface nanoscale axial photonics (SNAP) microresonators by the femtosecond (fs) laser post-processing technique for the first time. The internal stress can be induced by fs laser inscriptions in the fiber, causing nanoscale effective radius variation (ERV). However, the obtained ultra-precise fabrication usually undergoes multiple tries. Here, we propose a novel post-processing technique based on fs laser that significantly reduces the ERV errors and improves the fabrication precision without iterative corrections. The post-exposure process is achieved at the original exposure locations with using lower pulse energy than that in the initial fabrication process. The results show that the ERV is nearly proportional to the pulse energy of the post-exposure process. The slope of the ERV versus the pulse energy is 0.07 Å/nJ. The maximum of the post-processed ERV can reach 8.0 Å. The repeatability was experimentally verified by accomplishing the correction on three SNAP microresonators with the precision of 0.75 Å. The developed fabrication technique with fs laser enables SNAP microresonators with new breakthrough applications for optomechanics and filters. © 2018 Optical Society of America

OCIS codes: (060.2340) Fiber optics components; (230.3990) Micro-optical devices; (140.3945) Microcavities; (320.2250) Femtosecond phenomena

<http://dx.doi.org/10.1364/OL.99.099999>

The ultra-low propagation loss and remarkable fabrication precision of miniature photonic integrated circuits are always vital to the future practical microphotonic technology. However, the fabrication precision achieved in photonic devices and circuits

[1,2] is still changeable for the practical applications [3,4]. Surface nanoscale axial photonics (SNAP) has been proposed as a technological platform enabling fabrication of complex miniature photonic circuits at the smooth surface of an optical fiber with unprecedented sub-angstrom accuracy and ultralow loss [5,6]. This technology allows us to fabricate a series of microresonators along the optical fiber by introducing small nanoscale effective radius variation (ERV) [6-8]. The whispering gallery modes (WGMs) circulate circumferentially around the surface of the fiber while undergoing slow propagation along the fiber axis, which can be described by the one-dimensional Schrodinger equation [6]. The SNAP platform offers a new approach to practical microphotonic technology for optical communications, microwave photonics and quantum computing [5, 9-11]. Several works on the fabrication and applications of SNAP microresonators have been reported, such as bottle resonator delay lines [9], buffers [10] and optofluidic microresonators [11].

SNAP circuits are usually fabricated by local annealing of the optical fiber with a CO₂ laser or UV laser [7,22], which releases the tension frozen in the fiber during manufacture and leads to nanoscale radius variation. Due to the large mode area of the focused CO₂ laser beam as well as the limited photosensitivity of the fiber in the UV laser fabrication [7], it is difficult to get the SNAP circuits with both higher axial resolution and large ERV, which is significant for the practical miniature SNAP devices. Recently, femtosecond (fs) laser direct writing technology has been found numerous advantages in ultra-fine fabrication [12-14]. It demonstrated that SNAP microresonators can be introduced by the fs laser inscriptions with sub-angstrom precision [15]. This powerful technology is flexible and does not rely on the relaxation of the residual stress, enabling the fabrication in various types of materials [12]. Most importantly, due to the strong electromagnetic field of the ultra-short fs pulse, nonlinear interaction is involved in the fs laser microfabrication. By use of a nonlinear-optical process in the medium, the optical interaction can be

confined in a micrometer-sized focal volume [18,21]. Therefore, the modified zone induced by the fs laser inside the fiber could be smaller than the size of light spot on the surface of the fiber, which ensures the potential in fabricating predetermined shapes of SNAP microresonators with ultra-precision.

However, the sub-angstrom fabrication precision of SNAP circuits can only be obtained after multiple tries, which is due to the intrinsic nonuniformity of the fiber radius, surface contamination, imperfect system alignment and the fluctuations of the fs laser power. A correction method has been developed for the reduction of fabrication errors by multiple iterations with CO₂ laser shots [16]. Notably, to our best knowledge, no relative work has been reported in reducing the ERV errors by fs laser technology. Considering the fabrication advantages of fs lasers, we think a superior post-processing technique for the SNAP fabrication with the fs laser is needed, which is significant for the advancement of the ultraprecise SNAP fabrication platform.

In this paper, it is firstly experimentally demonstrated the correction of SNAP microresonators by fs laser post-processing technique. The post-exposure process is implemented on the original exposure locations with lower pulse energy. The results show that the ERV is nearly proportional to the pulse energy of the post-exposure process, which can effectively reduce the ERV errors without iterative corrections. The repeatability was experimentally verified by accomplishing the correction on three SNAP microresonators with sub-angstrom precision.

In our experiments, fs laser pulses ($\lambda=520$ nm) with 350 fs duration at the repetition rate of 200 kHz were focused into an optical fiber with 40 μm radius through an oiled objective lens (Olympus UMPLFL 63 \times) with a numerical aperture (NA) of 1.4. Stress rods of specific axial lengths were inscribed periodically and spaced by switching the laser on and off which is schematically shown in Fig. 1. The translation speed of the fiber was 20 $\mu\text{m}/\text{s}$, which can be adjusted with different axial inscription lengths and different laser repetition rates. Specifically, we introduced the internal stress by inscribing 9 parallel lines with an interval Δy of 4 μm , enabling the formation of the nanoscale ERV of an optical fiber. To characterize a SNAP microresonator, a biconical optical fiber taper with a waist diameter of ~ 1 μm was perpendicular to the SNAP fiber. The taper was connected to a tunable laser and a detector, translating along the SNAP fiber periodically touching it in 3 μm steps. The resonant transmission spectra were measured with 1 pm wavelength resolution at 1.55 μm (Fig. 1).

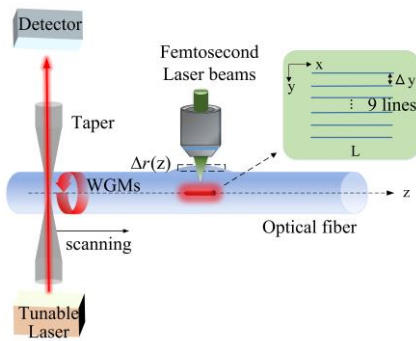


Fig. 1. Illustration of the setup of the nanoscale ERV introduced by fs laser inscriptions inside an optical fiber. The WGMs in the microresonators are excited by a transverse fiber taper. Inset shows the magnified profile of the inscription tracks.

To demonstrate a feasible calibration scheme, firstly, fs laser beams with the pulse energy of 97.5 nJ and repetition rate of 200 kHz were focused on the middle of an optical fiber. Five SNAP microresonators were fabricated with the same axial length of 250 μm inscriptions. The separation between adjacent microresonators is 100 μm . Figure 2(a) shows the microscope of the axial section of one microresonator in the initial fabrication process. The SNAP fiber is characterized by the microfiber scanning method after the fabrication. Figure 3(a) shows the surface plot of the transmission amplitude spectra of five SNAP microresonators in the initial fabrication process. In Fig. 3, the ERV Δr (right axis) is rescaled from the wavelength variation $\Delta\lambda$ (left axis) using the relation [17]

$$\Delta r = \frac{\Delta\lambda}{\lambda_0} \cdot r_0, \quad (1)$$

where the fiber radius $r_0 = 40$ nm and wavelength $\lambda_0 = 1553$ nm. The ERVs of microresonators with same fabrication parameters are 16.718 nm, 15.534 nm, 16.602 nm, 15.315 nm, 16.178 nm, respectively [Fig. 3(a)]. The ERV deviations may be caused by the surface contamination and intrinsic nonuniformity of the fiber radius. Due to the expansion of the induced stress during the fs laser beams exposure, the spacing between two SNAP microresonators is smaller than 100 μm . However, we have checked that the adjacent microresonators are not coupled to each other. Thus, it does not affect the following analysis of the ERV characteristics.

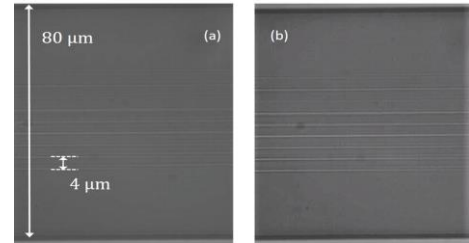


Fig. 2. Microscope images of the axial section of one microresonator inscribed with 9 parallel lines, which was fabricated in (a) the initial fabrication and (b) the calibrated fabrication. The pulse energy of 62.5 nJ was utilized to calibrate the microresonator in (b).

Then, the fabricated SNAP fiber in the initial fabrication process was put back onto the fs laser fabrication platform. Five SNAP microresonators were separately post-processed on their own original exposure locations. However, the pulse energy on the five SNAP microresonators were 21.7 nJ, 28.5 nJ, 38.8 nJ, 45.5 nJ and 62.5 nJ from left to right in the SNAP fiber, respectively, which were lower than those in their initial process. Notably, since the ERV errors caused by the nonuniformity of the fiber in the initial fabrication is small, as we can get from Fig. 3(a), the lower pulse energy in the calibrated fabrication is used to induce the smaller ERV which is appropriate for correcting the smaller ERV errors.

Figure 2(b) shows the micrographs of the inscribed lines in the calibrated fabrication. The lines in Fig. 2(b) is clearer than those in Fig. 2(a), due to the more intensive modulation and internal stress induced in the calibrated fabrication. The transmission amplitude spectra of the five SNAP microresonators in the calibrated fabrication are given in Fig. 3(b). The local ERVs of microresonators are 16.988 nm, 15.881 nm, 17.014 nm, 15.779 nm, 16.731 nm, respectively. Comparing the ERVs in Fig. 3(a) and

3(b), it indicates that the ERV of each microresonator increases differently because of the different energies of laser pulses used in the calibrated fabrication.

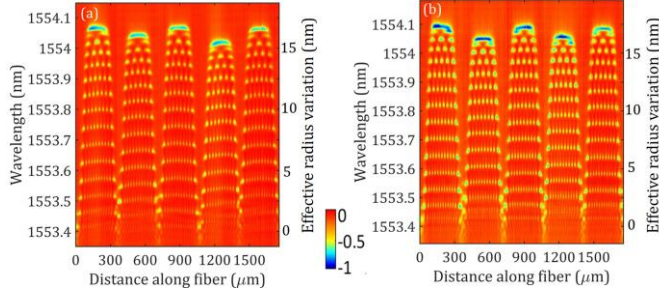


Fig. 3. Surface plots of the resonant transmission amplitude spectra of (a) the initial fabrication process and (b) the calibrated fabrication. The surface plots of experimental data are obtained with 1.0 pm resolution in wavelength and 3 μm resolution along the fiber axis.

In order to evaluate the change of the ERV quantitatively in Fig. 3, ERVs of five SNAP microresonators in the initial fabrication and the calibrated fabrication are compared respectively. Curves 1 and 2 in Fig. 4 show the total ERVs of the five microresonators corresponding to Fig. 3(a) and Fig. 3(b), respectively. The curve 3 in Fig. 4 represents the difference between the initial and calibrated fabrication. Here, the increase of ERV is caused by the calibrated fabrication, which is nearly proportional to the pulse energy in the calibrated fabrication. The slope of the increase of ERV versus the pulse energy is 0.07 Å/nJ. The maximum of the ERV in the calibrated fabrication can reach 8.0 Å, which is limited by the pulse energy in the initial fabrication.

To explain the results above, it is necessary for us to review the mechanism of the fs laser fabrication. For such relevant physical process of fs laser pulses, the nonlinear interaction between the fs pulse and transparent materials spends only a couple of microseconds. Within a few nanoseconds, a pressure or a shock wave separates from the dense and hot focal volume. The high energy diffuses out of the focal volume in several microseconds. The expanding material in the irradiated zone induces strain in the vicinity of the track and permanent refractive index modulation [14,18]. Meanwhile, considering the effect of the induced stress on the nanoscale ERV on an optical fiber surface, the ERV can be estimated through the Lamé's equation for a thick-walled cylinder [15,19] as follows:

$$\Delta r = 2r_i^2 P_i / E r_0, \quad (2)$$

where r_i is the radius of the fabrication area, r_0 is that of the fiber, E is the Young modulus of silica, P_i is the pressure introduced by the fs laser inscriptions. It obviously shows in Eq. (2) that the ERV is proportional to P_i , which means that the ERV grows as the induced stress increases. Furthermore, with the combination of the experimental results in curve 3, we speculate that the induced stress is presumably proportional to the pulse energy within a certain range, where the pulse energy in the calibrated fabrication is lower than that of the initial fabrication.

Remarkably, the curve 3 in Fig. 4 indicates that the increase of the ERV is controllable and can be used to

compensate the ERV errors in the initial fabrication. Although the maximum of the tuning ERV in the calibrated fabrication is 8.0 Å, which is smaller than that of the CO₂ laser [16]. However, it is more flexible for correcting smaller ERV errors with fs laser. Additionally, this post-exposure process takes only once without multiple correction processes, which is relatively simple and flexible.

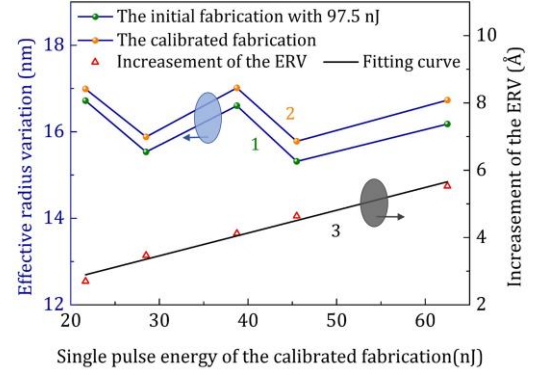


Fig. 4. The plot of the ERVs characterizing the five SNAP microresonators. Curves 1 and 2 show the ERVs of the five microresonators corresponding to Fig. 3(a) and Fig. 3(b), respectively. The red points show the difference of ERV between curves 1 and 2. Curve 3 (black line) gives the best linear fitting $\Delta \text{ERV} = 0.07E + 1.175$ with the linearity of 0.98.

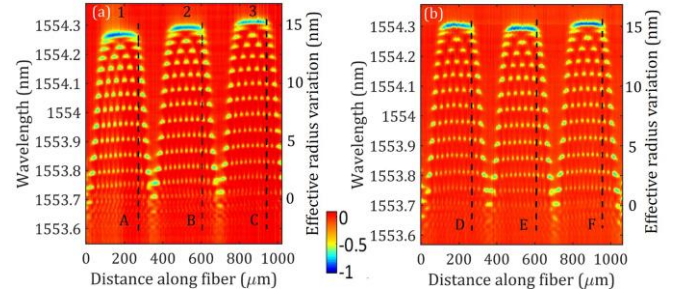


Fig. 5. Surface plots of the resonant transmission amplitude spectra of that (a) before the correction and (b) after the correction. The spectra at positions A, B, C, D, E and F, which are separately chosen at each microresonator, are compared in Fig. 6.

According to the calibration scheme, we made the corrections. Three new SNAP microresonators were fabricated with the same inscription parameters as those in Fig. 3(a). Figure 5(a) presents the transmitted spectra of SNAP microresonators in the initial fabrication. It is calculated that the three SNAP microresonators have the maximal ERV errors of 0.27 Å. To equalize them, we chose the pulse energy of 82.5 nJ and 36 nJ for microresonators 1 and 2, respectively, according to their deviations from the microresonator 3 and the calibrated results given in Fig. 4. Figure 5(b) shows the resultant spectral plot of remarkably uniform microresonators after the correction. The total ERVs of microresonators 1, 2 are nearly equal to the microresonator 3. The

results in Fig. 5 forcefully confirm the repeatability and reliability of our proposed correction scheme with fs laser.

To estimate the fabrication precision of SNAP microresonators based on the proposed analysis method in [17], we chose and compared the relative positions of narrowest spectral lines at the same position (such as A, B and C) of different microresonators. The spectra of the locations marked in Fig. 5 are shown in Fig. 6. The local enlargements of the marked portions in Fig. 6(a) and 6(b) are shown in Fig. 6(c) and 6(d), respectively. The maximum deviation of resonance wavelength shifts is reduced from 27 pm to 2 pm, corresponding to the ERV errors from 6.9 Å to 0.5 Å. We note that the transmission variation in Fig. 6(c) and 6(d) shows the change of coupling ratio, which is caused by the small difference of the coupling distance in the initial and corrected measurements. However, it doesn't affect the conclusion of our experiments. It demonstrates that the correction scheme based on fs laser makes unique performance on improving the fabrication precision by over an order of magnitude. The precision of our measurements is limited to 0.25 Å, which depends on the resolution of our measurement system. Generally, the temperature effect is negligible due to the offered stable and closed experiment environment. Therefore, the summarized fabrication precision of the SNAP micro-resonator is approximated below ~ 0.75 Å. It is the first demonstration of the sub-angstrom precision correction of SNAP microresonators with the fs laser post-processing technique.

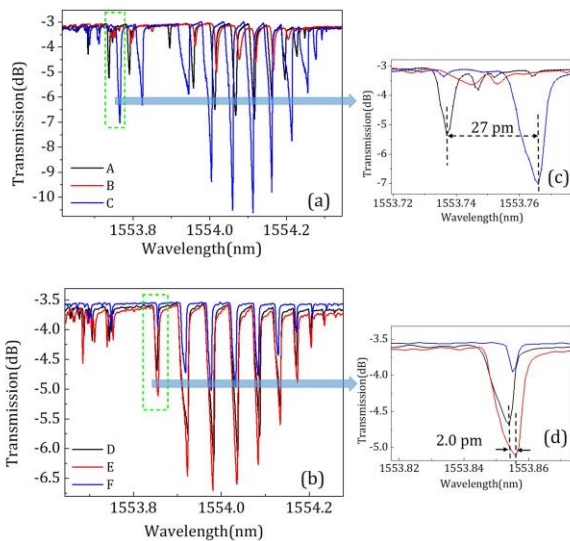


Fig. 6. The spectra analysis of fabrication precision by comparing the spectra of three SNAP microresonators. (a) Spectra of three SNAP microresonators presented in Fig. 5(a) at positions A, B and C. (b) Spectra of three SNAP microresonators presented in Fig. 5(b) at positions D, E and F. (c), (d) The enlarged spectra of the green dotted line in (a) and (b).

In summary, we have demonstrated the correction of SNAP microresonators by fs laser post-processing technique. The method is based on the post-exposure process at the original exposure locations with lower pulse energy. The results show that

the ERV is proportional to the pulse energy in the post-exposure process. It can flexibly compensate the fabrication errors in the initial fabrication with sub-angstrom precision. Our experimental results also demonstrate that the induced stress in the fiber is nearly proportional to the pulse energy within a certain range, which contributes to the literatures of fs fabrication. Furthermore, since the maximum of post-processed ERV is 8.0 Å, which is smaller than the result previously achieved in [16], further study will focus on improving the corrected range. It could be achieved by increasing the pulse energy of the post-exposure process to be higher than that of the initial fabrication. However, the linearity of the ERV versus the pulse energy in this region needs to be further investigated. What's more, a more complete corrected range can also be performed by increasing the strength of the introduced stress in the post-exposure process, such as increasing the number of inscription lines [20], inscription areas, and so on. Overall, the fs laser post-processing technique can be potentially developed into a very useful and powerful correction technique for SNAP microresonators fabrication, paving the way to its applications for optomechanics and filters.

Funding. National Natural Science Foundation of China (NSFC) (61775074); National 1000 Young Talents Program, China; 111 Project (No. B07038).

References

- W. Bogaerts, P. De Heyn, T. Van Vaerenbergh, K. DeVos, S. K. Selvaraja, T. Claes, P. Dumon, P. Bienstman, D. Van Thourhout, and R. Baets, *Laser Photon. Rev.* **6**, 47 (2012).
- F. N. Xia, L. Sekaric, and Y. Vlasov, *Nat. Photon.* **1**, 65 (2007).
- Y. Li, A. V. Maslov, I. L. Nicholas, M. U. Augustine, V.N. Astratov, *Laser & Photonics Rev.* **9**, 263 (2015).
- L. Tong, R. R. Gattass, J. B. Ashcom, S. He, J. Lou, M. Shen, I. Maxwell, E. Mazur, *Nature*, **42** (2003).
- M. Sumetsky, *Nanophotonics* **2**, 393 (2013).
- M. Sumetsky and J. M. Fini, *Opt. Express* **19**, 26470 (2011).
- M. Sumetsky, D. J. DiGiovanni, Y. Dulashko, J. M. Fini, X. Liu, E. M. Monberg, and T. F. Taunay, *Opt. Lett.* **36**, 4824 (2011).
- M. Sumetsky, K. Abedin, D. J. DiGiovanni, Y. Dulashko, J. M. Fini, and E. M. Monberg, *Opt. Lett.* **37**, 990 (2012).
- M. Sumetsky, *Phys. Rev. Lett.* **111**, 163901 (2013).
- M. Sumetsky, *Sci. Rep.* **5**, 18569 (2015).
- T. Hamidfar, K. V. Tokmakov, B. J. Mangan, R. S. Windeler, A. V. Dmitriev, D. L. P. Vitullo, P. Bianucci, and M. Sumetsky, *optica* **5**, 382 (2018).
- R. R. Gattass and E. Mazur, *Nat. photon.* **2**, 219 (2008)
- M. Beresna, M. Gecevičius, and P. G. Kazansky, *Adv. Opt. Photon.* **6**, 293 (2014).
- J. R. Grenier, L. A. Fernandes, and P. R. Herman, *Opt. Express* **23**, 16760 (2015).
- F. Shen, X. Shu, L. Zhang and M. Sumetsky, *Opt. Lett.* **41**, 2795 (2016).
- M. Sumetsky and Y. Dulashko, *Opt. Express* **20**, 27896(2012).
- N. A. Toropov and M. Sumetsky, *Opt. Lett.* **41**, 2278(2016).
- M Sakakura, M. Terazima, Y. Shimotsuma, K. Miura, and K. Hirao, *Opt. Express* **15**, 5674 (2007).
- S. P. Timoshenko and J. N. Goodier, *Theory of Elasticity*, 3rd ed. (McGraw-Hill, 1970).
- Q. Yu, F. Shen, Z. Xu, H. Cao, M. Sumetsky and X. Shu, *CLEO: QELS_Fundamental Science* (Optical Society of America, 2018), JW2A.
- S. Kawata, H. B. Sun, T. Tanaka, and K. Takada, *Nature* **412**, 697 (2001).
- M. Sumetsky, D. J. DiGiovanni, Y. Dulashko, X. Liu, E. M. Monberg, and T. F. Taunay, *Opt. Express* **20**, 10685(2012).

References

1. W. Bogaerts, P. De Heyn, T. Van Vaerenbergh, K. DeVos, S. K. Selvaraja, T. Claes, P. Dumon, P. Bienstman, D. Van Thourhout, and R. Baets, "Silicon microring resonators," *Laser Photon. Rev.* **6**, 47-73 (2012).
2. F. N. Xia, L. Sekaric, and Y. Vlasov, "Ultracompact optical buffers on a silicon chip," *Nat. Photon.* **1**, 65 (2007).
3. Y. Li, A.V. Maslov, I. L. Nikolaos, M. U. Augustine, V.N. Astrato, "Spectrally Resolved Resonant Propulsion of Dielectric Microspheres," *Laser & Photonics Rev.* **9**, 263–273 (2015).
4. L. Tong, R. R. Gattass, J. B. Ashcom, S. He, J. Lou, M. Shen, I. Maxwell, E. Mazur, "Subwavelength-diameter silica wires for low-loss optical wave guiding," *Nature* **426**, 816 (2003).
5. M. Sumetsky, "Nanophotonics of optical fibers," *Nanophotonics* **2**, 393-406 (2013).
6. M. Sumetsky and J. M. Fini, "Surface nanoscale axial photonics," *Opt. Express* **19**, 26470-26485 (2011).
7. M. Sumetsky, D. J. DiGiovanni, Y. Dulashko, J. M. Fini, X. Liu, E. M. Monberg, and T. F. Taunay, "Surface nanoscale axial photonics: robust fabrication of high-quality-factor microresonators," *Opt. Lett.* **36**, 4824-4826 (2011).
8. M. Sumetsky, K. Abedin, D. J. DiGiovanni, Y. Dulashko, J. M. Fini, and E. M. Monberg, "Coupled high Q-factor surface nanoscale axial photonics (SNAP) microresonators," *Opt. Lett.* **37**, 990-992 (2012).
9. M. Sumetsky, "Delay of light in an optical bottle resonator with nanoscale radius variation: dispersionless, broadband, and low loss," *Phys. Rev. Lett.* **111**, 163901 (2013).
10. M. Sumetsky, "Microscopic optical buffering in a harmonic potential," *Sci. Rep.* **5**, 18569 (2015).
11. T. Hamidfar, K. V. Tokmakov, B. J. Mangan, R. S. Windeler, A. V. Dmitriev, D. L. P. Vitullo, P. Bianucci, and M. Sumetsky, "Localization of light in an optical microcapillary induced by a droplet," *optica* **5**, 382-388 (2018).
12. R. R. Gattass and E. Mazur, "Femtosecond laser micromachining in transparent materials," *Nat. photon.* **2**, 219 (2008).
13. M. Beresna, M. Gecevičius, and P. G. Kazansky, "Ultrafast laser direct writing and nanostructuring in transparent materials," *Adv. Opt. Photon.* **6**, 293-339 (2014).
14. J. R. Grenier, L. A. Fernandes, and P. R. Herman, "Femtosecond laser inscription of asymmetric directional couplers for in-fiber optical taps and fiber cladding photonics," *Opt. Express* **23**, 16760-16771 (2015).
15. F. Shen, X. Shu, L. Zhang and M. Sumetsky, "Fabrication of surface nanoscale axial photonics structures with a femtosecond laser," *Opt. Lett.* **41**, 2795-2798 (2016).
16. M. Sumetsky and Y. Dulashko, "SNAP: Fabrication of long coupled microresonator chains with sub-angstrom precision," *Opt. Express.* **20**, 27896-27901(2012).
17. N. A. Toropov and M. Sumetsky, "Permanent matching of coupled optical bottle resonators with better than 0.16 GHz precision," *Opt. Lett.* **41**, 2278-2281 (2016).
18. M. Sakakura, M. Terazima, Y. Shimotsuma, K. Miura, and K. Hirao, "Observation of pressure wave generated by focusing a femtosecond laser pulse inside a glass," *Opt. Express* **15**, 5674-5686 (2007).
19. S. P. Timoshenko and J. N. Goodier, *Theory of Elasticity*, 3rd ed. (McGraw-Hill, 1970).
20. Q. Yu, F. Shen, Z. Xu, H. Cao, M. Sumetsky and X. Shu, "Tuning effective fiber radius variation of SNAP structures with a femtosecond laser," *CLEO: QELS_Fundamental Science* (Optical Society of America, 2018), JW2A.
21. S. Kawata, H. B. Sun, T. Tanaka, and K. Takada, "Finer features for functional microdevices," *Nature* **412**, 697–698 (2001).
22. M. Sumetsky, D. J. DiGiovanni, Y. Dulashko, X. Liu, E. M. Monberg, and T. F. Taunay. "Photo-induced SNAP: fabrication, trimming, and tuning of microresonator chains," *Opt. Express* **20**, 10684-10691(2012).